JOURNAL OF MATERIALS SCIENCE 31 (1996) 4105–4110

Application of homogenization FEM analysis to regular and re-entrant honeycomb structures

JINHEE LEE
Department of Mechanical Engineering, Hong-ik University, Chochiwon, Yeongi-gun, Chungnam 339-800, Korea

J. B. CHOI*, K. CHOI*
Biomedical Research Center, Korea Institute of Science and Technology, PO Box 131, Cheongryang, Seoul 130-650, Korea

Honeycomb structures are widely used in structural applications because of their high strength per density. Re-entrant honeycomb structures with negative Poisson's ratios may be envisaged to have many potential applications. In this study, an homogenization finite element method (FEM) technique developed for the analysis of spatially periodic materials is applied for the analysis of linear elastic responses of the regular and re-entrant honeycomb structures. Young's modulus of the regular honeycomb increased with volume fraction. Poisson's ratio of the regular honeycomb structure decreased from unity as volume fraction increased. The re-entrant honeycomb structure had a negative Poisson's ratio, its value dependent upon the inverted angle of cell ribs. Young's modulus of the re-entrant honeycomb structure decreased as the inverted angle of cell ribs increased. The results are in good agreement with previous analytical results. This homogenization theory is also applicable to three-dimensional foam materials – conventional and re-entrant.

Nomenclature

b_i	Body force
E, E_{ijkl}	Young's modulus, elasticity tensor
E_e	Effective Young's modulus
E^H_{ijkl}	Homogenized elasticity tensor
t_i	Traction
$u_i, \underline{u}$	Displacement
$v_i, \underline{v}$	Virtual displacement
$x_i, \underline{x}$	Macroscale coordinate
$y_i, \underline{y}$	microscale coordinate
ε	Microscopic/macroscopic ratio
ϕ	Volume fraction
ν	Poisson's ratio
ν_e	Effective Poisson's ratio
σ_{ij}	Stress
χ_p^{kl}	Microscale parameter of separation of variables

1. Introduction

Cellular materials are multiphase composite material systems that consist of a solid matrix and a fluid phase, the fluid usually being a gas. Morphologically, cellular solids are classified into two-dimensional solids such as a honeycomb structure which contains hexagonal cells and three-dimensional foams such as sponge. These cellular solids are increasingly used structurally because of their high strength combined with being lightweight. In two-dimensional cellular materials, if the polygon which packs to fill a plane area is regular, these materials can be treated as having a special symmetric behaviour in plane, for example, transversely isotropic with a regular hexagon (Fig. 1).

Poisson's ratio, ν, describes a dimensional change in lateral direction to longitudinal direction when a force is applied in a longitudinal direction. It is possible to have materials that become fatter when stretched because the positive strain energy theory of isotropic elasticity allows Poisson's ratios in the range from -1 to $1/2$ [1]. But isotropic materials with negative Poisson's ratios have not been reported. Recently, isotropic polymer [2] and metallic [3] foams with negative Poisson's ratios were developed by a cell shape change from a convex polyhedron to a concave (i.e. bulges inwards) one. One can easily observe the rationale of negative Poisson's ratios: suppose that one crumples a plain piece of paper and stretches it from opposite corners, then the paper expands laterally. In addition to the negative Poisson's ratio, this new material showed enhancements in several material properties such as impact absorption, damage resistance, damage tolerance, plane strain fracture toughness, resilience, shearing modulus and indentation resistance, compared to the conventional foam materials with positive Poisson's ratios [2, 3].

Meanwhile, the conventional honeycomb structure can be fabricated to have a negative Poisson's ratio

*Author to whom all correspondence should be addressed.

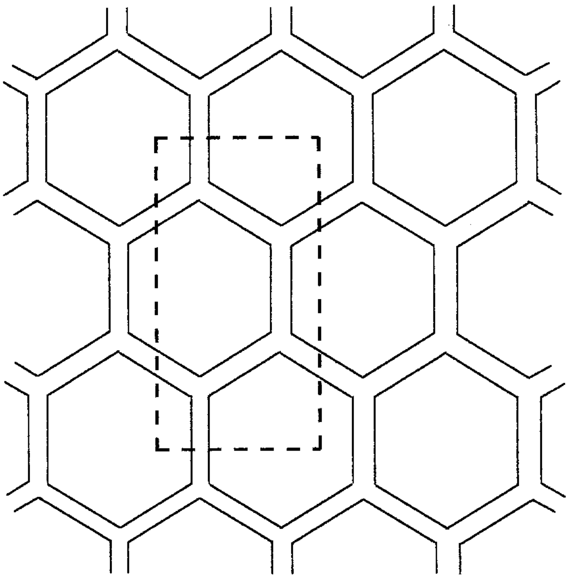

Figure 1 A conventional honeycomb structure with regular hexagonal cells; dashed rectangle, repeating unit.

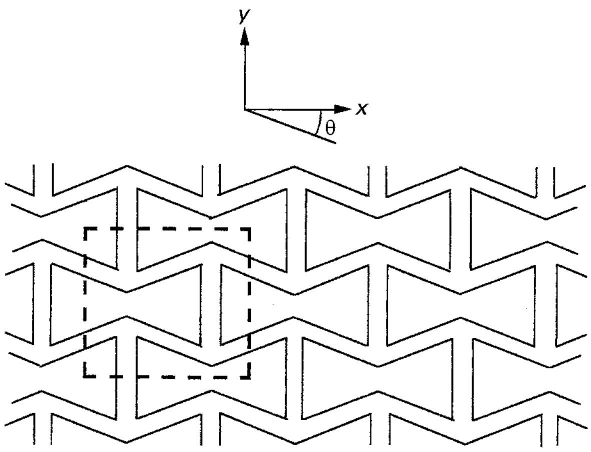

Figure 2 A re-entrant honeycomb structure with inverted cells; dashed rectangle, repeating unit.

(Fig. 2). Honeycomb structures with inverted (re-entrant) cells have been reported to have negative Poisson's ratios in the cell plane [4, 5]. The linear elastic response of these honeycomb structures – conventional and re-entrant – has recently been obtained via a structural analysis in repeating volume element [6, 7] and a beam analysis of the unit cell [8]. It was proposed that effective elastic moduli, effective Young's modulus and effective Poisson's ratio, depend on the volume fraction, ϕ, which is the ratio of matrix volume to whole volume. The re-entrant honeycomb structures with negative Poisson's ratios may be useful in many potential applications which take advantage of the above enhanced properties. Several anisotropic materials are known to have negative Poisson's ratios. These include a few natural single crystals [9], some composite laminates [10], microporous polytetrafluoroethylene (PTFE) [11] and microporous ultra-high molecular weight polyethylene [12].

FEM has gained in popularity as one of the most powerful tools in the area of stress analysis. However, a close look at the cellular material microstructure reveals that it is extremely difficult to analyse such a structure at the level of individual microstructural units. Conventional FEM assumes material homogeneity and isotropy, and it is apparent that such assumptions are hardly applicable because of the high degree of material heterogeneity. One of the reasonable ways to overcome this difficulty is to find an equivalent material model without a need to represent every individual microstructural unit.

There have been enormous efforts to compute various effective material properties of composite materials, as can be seen in Hashin's survey [13]. Most of the methods, however, are hardly applicable, except to simple geometries such as the composite sphere assemblage (CSA) and the composite cylinder assemblage (CCA). The homogenization theory, which introduces asymptotic expansion to standard FEM, helps find such a material model for spatially periodic materials which is able to characterize the average mechanical behaviour as well as represent the effect of the material heterogeneities [14, 15].

The purpose of this study is to analyse the linear elastic response of the conventional and re-entrant honeycomb structures by applying an homogenization FEM technique to the honeycomb structures. The results of the present study are compared to previous analytical results. If this technique does work on the two-dimensional cellular solid, honeycomb structure, it will be applied to three-dimensional foams – conventional and re-entrant – in future work.

2. Method

The finite element weak form of the linear elasticity problems is given by

$$\int_\Omega E_{ijkl} \frac{\partial u_k}{\partial x_l} \frac{\partial v_i}{\partial x_j} \, \mathrm{d}\Omega = \int_\Omega b_i v_i \, \mathrm{d}\Omega + \int_\Gamma t_i v_i \, \mathrm{d}\Gamma \quad (1)$$

In homogenization theory, the field variables, including virtual displacements, are expressed as asymptotic expansions with respect to the parameter $\varepsilon\,(|\varepsilon| \ll 1)$ such that

$$\underline{u} = \underline{u}^0(\underline{x}) + \varepsilon\, \underline{u}^1(\underline{x}, \underline{y}) + \mathrm{O}(\varepsilon^2) \quad (2)$$

$$\underline{v} = \underline{v}^0(\underline{x}) + \varepsilon\, \underline{v}^1(\underline{x}, \underline{y}) + \mathrm{O}(\varepsilon^2) \quad (3)$$

hold, where $\underline{y} = \underline{x}/\varepsilon$ is the microscale coordinate. The gradients of $\underline{u}$ and $\underline{v}$ are given by

$$\nabla \underline{u} = \nabla_{\underline{x}} \underline{u}^0 + \varepsilon \nabla_{\underline{x}} \underline{u}^1 + \nabla_{\underline{y}} \underline{u}^1 \quad (4)$$

$$\nabla \underline{v} = \nabla_{\underline{x}} \underline{v}^0 + \varepsilon \nabla_{\underline{x}} \underline{v}^1 + \nabla_{\underline{y}} \underline{v}^1 \quad (5)$$

Substituting Equations 2–5 into Equation 1 and rearranging gives

$$\begin{aligned}
&\int_\Omega E_{ijkl} \left(\frac{\partial u_k^0}{\partial x_l} + \frac{\partial u_k^1}{\partial y_l} \right) \left(\frac{\partial v_i^0}{\partial x_j} + \frac{\partial v_i^1}{\partial y_j} \right) \mathrm{d}\Omega \\
&\quad + \varepsilon \int_\Omega E_{ijkl} \left[\frac{\partial u_k^1}{\partial x_l} \left(\frac{\partial v_i^0}{\partial x_j} + \frac{\partial v_i^1}{\partial y_j} \right) \right. \\
&\quad \left. + \left(\frac{\partial u_k^0}{\partial x_l} + \frac{\partial u_k^1}{\partial y_l} \right) \frac{\partial v_i^1}{\partial x_j} \right] \mathrm{d}\Omega + \varepsilon^2 \int_\Omega E_{ijkl} \frac{\partial u_k^1}{\partial x_l} \frac{\partial v_i^1}{\partial x_j} \, \mathrm{d}\Omega \\
&= \int_\Omega b_i (v_i^0 + \varepsilon v_i^1) \, \mathrm{d}\Omega + \int_\Gamma t_i (v_i^0 + \varepsilon v_i^1) \, \mathrm{d}\Gamma \quad (6)
\end{aligned}$$

Taking the limit of $\varepsilon \to 0$ reduces Equation 6 to

$$\lim_{\varepsilon \to 0} \int_{\Omega} E_{ijkl} \left(\frac{\partial u_k^0}{\partial x_l} + \frac{\partial u_k^1}{\partial y_l} \right) \left(\frac{\partial v_i^0}{\partial x_j} + \frac{\partial v_i^1}{\partial y_j} \right) \mathrm{d}\Omega$$

$$= \lim_{\varepsilon \to 0} \left[\int_{\Omega} b_i v_i^0 \, \mathrm{d}\Omega + \int_{\Gamma} t_i v_i^0 \, \mathrm{d}\Gamma \right] \quad (7)$$

Since the virtual displacement $\underline{v} = \underline{v}^0 + \varepsilon \underline{v}^1$ is arbitrary, it turns out that $\underline{v}^0$ and $\underline{v}^1$ are also arbitrary and Equation 7 is rewritten as

$$\lim_{\varepsilon \to 0} \int_{\Omega} E_{ijkl} \left(\frac{\partial u_k^0}{\partial x_l} + \frac{\partial u_k^1}{\partial y_l} \right) \frac{\partial v_i^0}{\partial x_j} \mathrm{d}\Omega$$

$$= \lim_{\varepsilon \to 0} \left[\int_{\Omega} b_i v_i^0 \, \mathrm{d}\Omega + \int_{\Gamma} t_i v_i^0 \, \mathrm{d}\Gamma \right] \quad (8)$$

and

$$\lim_{\varepsilon \to 0} \int_{\Omega} E_{ijkl} \left(\frac{\partial u_k^0}{\partial x_l} + \frac{\partial u_k^1}{\partial y_l} \right) \frac{\partial v_i^1}{\partial y_j} \mathrm{d}\Omega = 0 \quad (9)$$

It is readily seen that Equations 8 and 9 are not independent, rather they are mutually dependent through the term $(\partial u_k^0/\partial x_l) + (\partial u_k^1/\partial y_l)$.

Considering that the microscale integration can be replaced by an averaged value integration for a general Y periodic function Φ

$$\lim_{\varepsilon \to 0} \int_{\Omega} \Phi(\underline{x}, \underline{y}) \, \mathrm{d}\Omega = \int_{\Omega} \frac{1}{|Y|} \int_{Y} \Phi(\underline{x}, \underline{y}) \, \mathrm{d}Y \, \mathrm{d}\Omega \quad (10)$$

Equations 8 and 9 are now modified to give

$$\int_{\Omega} \frac{1}{|Y|} \int_{Y} E_{ijkl} \left(\frac{\partial u_k^0}{\partial x_l} + \frac{\partial u_k^1}{\partial y_l} \right) \frac{\partial v_i^0}{\partial x_j} \mathrm{d}Y \, \mathrm{d}\Omega$$

$$= \int_{\Omega} b_i v_i^0 \, \mathrm{d}\Omega + \int_{\Gamma} t_i v_i^0 \, \mathrm{d}\Gamma \quad (11)$$

and

$$\int_{\Omega} \frac{1}{|Y|} \int_{Y} E_{ijkl} \left(\frac{\partial u_k^0}{\partial x_l} + \frac{\partial u_k^1}{\partial y_l} \right) \frac{\partial v_i^1}{\partial y_j} \mathrm{d}Y \, \mathrm{d}\Omega = 0 \quad (12)$$

Considering the linear relationship, the following separation of variables is a sufficient condition to satisfy Equation 12

$$u_i^1(\underline{x}, \underline{y}) = -\chi_i^{pq}(\underline{y}) \frac{\partial u_p^0(\underline{x})}{\partial x_q} \quad (13)$$

The microscale parameter χ_p^{kl} is computed by the substitution of Equation 13 into Equation 12

$$\int_{Y} \left(E_{ijkl} - E_{ijpq} \frac{\partial \chi_p^{kl}}{\partial y_q} \right) \frac{\partial v_i^1}{\partial y_j} \mathrm{d}Y \frac{\partial u_k^0}{\partial x_l} = 0 \quad (14)$$

Finally, the weak form of macroscale Equation 11 is rewritten as

$$\int_{\Omega} E_{ijkl}^{\mathrm{H}} \frac{\partial u_k^0}{\partial x_l} \frac{\partial v_i^0}{\partial x_j} \mathrm{d}\Omega = \int_{\Omega} b_i v_i^0 \, \mathrm{d}\Omega + \int_{\Gamma} t_i v_i^0 \, \mathrm{d}\Gamma \quad (15)$$

where the homogenized elasticity tensor E^{H} is computed by

$$E_{ijkl}^{\mathrm{H}} = \frac{1}{|Y|} \int_{Y} \left(E_{ijkl} - E_{ijpq} \frac{\partial \chi_p^{kl}}{\partial y_q} \right) \mathrm{d}Y \quad (16)$$

Repeating units were chosen from the regular and re-entrant honeycomb structures, as can be seen in Figs 1 and 2, and the homogenization technique was applied to those repeating units to compute the homogenized elasticity tensor, E^{H}. In the conventional honeycomb, the effect of volume fraction on Young's modulus and Poisson's ratio is investigated. In the re-entrant honeycomb, the same elastic properties are obtained by changing the inverted angle under the assumption of initial volume fraction of 0.1. Four different Poisson's ratios of 0, 0.1, 0.2 and 0.3 were used for the matrix material of the honeycomb structures throughout the computations.

The effective elastic modulus, E_{e}, and Poisson's ratio, ν_{e}, for each case were obtained from the plane stress assumption as follows

$$\begin{bmatrix} E_{1111}^{\mathrm{H}} & E_{1122}^{\mathrm{H}} & 0 \\ E_{2211}^{\mathrm{H}} & E_{2222}^{\mathrm{H}} & 0 \\ 0 & 0 & E_{1212}^{\mathrm{H}} \end{bmatrix}$$

$$= \frac{E_{\mathrm{e}}}{1 - \nu_{\mathrm{e}}^2} \begin{bmatrix} 1 & \nu_{\mathrm{e}} & 0 \\ \nu_{\mathrm{e}} & 1 & 0 \\ 0 & 0 & \frac{1 - \nu_{\mathrm{e}}}{2} \end{bmatrix} \quad (17)$$

3. Results and discussion

In the calculations of the effective Young's moduli and Poisson's ratios of the conventional and re-entrant honeycombs, we have used four different values of 0, 0.1, 0.2 and 0.3 as Poisson's ratio of the matrix material. The results showed almost the same values within 0.1% deviation, regardless of Poisson's ratio of the matrix material. Thus, it can be said that the linear elastic behaviour of honeycomb structures is independent of Poisson's ratio of the matrix material. The effective Young's modulus of honeycomb structures is linearly dependent upon Young's modulus of the matrix material. Since we are going to deal with the normalized Young's modulus, which is the ratio of the effective Young's modulus of the honeycomb structures to Young's modulus of the matrix material, the magnitude of Young's modulus of the matrix material does not affect the normalized Young's modulus. The magnitude is also independent of the effective Poisson's ratio of honeycomb structures. In the following discussion, only the results for a Poisson's ratio of 0.3 for the matrix material are described.

Fig. 3 shows the comparison of the present result with other analytical results in the effective Young's modulus of the conventional honeycomb with regular hexagons. As mentioned above, Warren and Kraynik [6] used a structural analysis in repeating volume element and Gibson and Ashby [8] applied a beam-bending analysis to a unit cell. Gibson and Ashby's result contained only a ϕ^3 term in its expression. But, Warren and Kraynik obtained a polynomial form of ϕ with ϕ^3 as the lowest order. Thus, the two analyses gave almost the same result at low density and E_{e}/E was proportional to ϕ^3. The effect of higher order terms increases at high volume fractions, as shown in

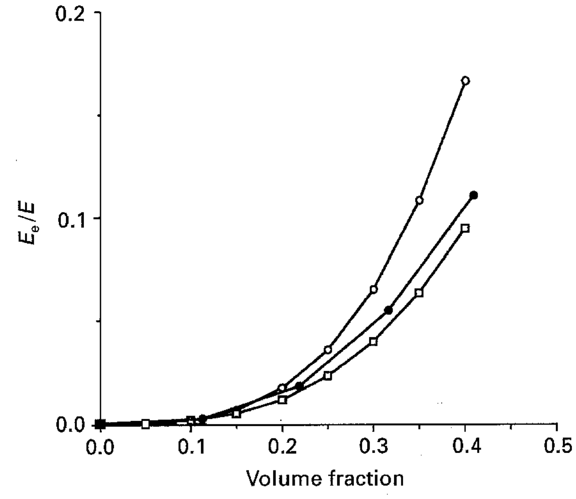

Figure 3 The dependence of the effective Young's modulus on volume fraction of the conventional honeycomb structure. ○, Warren and Kraynik [6]; □, Gibson and Ashby [8]; ●, present results.

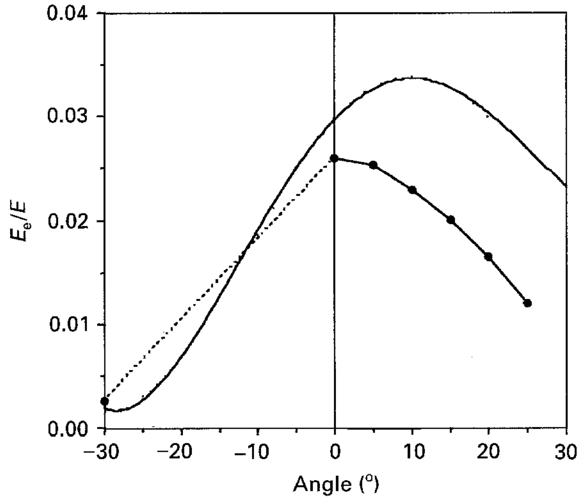

Figure 5 The relationship between the effective Young's modulus and the inverted angle of cell ribs with an initial volume fraction of 0.1; dotted line, no data available in the present results. ——, Warren [7]; -●- present results.

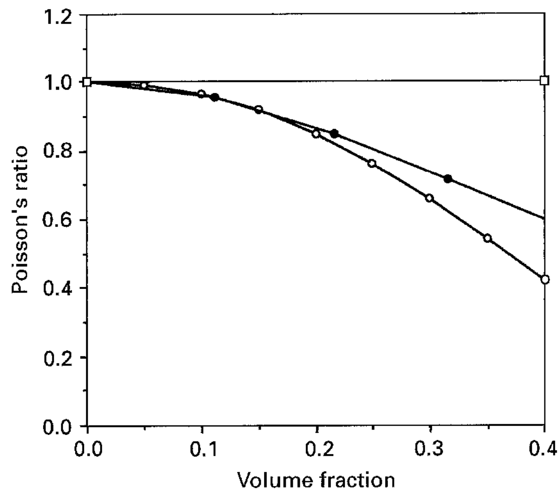

Figure 4 Effective Poisson's ratio versus volume fraction of the conventional honeycomb structure. ○, Warren and Kraynik [6]; □, Gibson and Ashby [8]; ●, present results.

Fig. 3. The result of the present study falls between the two analytical results over all volume fractions covered. Therefore, it can be said that the homogenization FEM technique works quite well on the two-dimensional cellular solid, honeycomb structure.

Fig. 4 shows the dependence of the effective Poisson's ratio of conventional honeycombs on volume fraction. Gibson and Ashby proposed a unit Poisson's ratio regardless of volume fraction. However, the present result, as well as Warren and Kraynik's result, shows its dependence on the volume fraction: the effective Poisson's ratio decreases from unity with increasing volume fraction. At low volume fraction, where bending is the primary deformation mechanism, the effective Poisson's ratio of conventional honeycombs approaches unity. At higher volume fractions, however, bending is no longer dominant and a considerable amount of axial extension or compression of cell ribs contributes to the deformation in the linear elastic region. Thus, the dependence of Poisson's ratio on volume fraction is more probable in cellular structures. This is further supported by the fact that the effective Poisson's ratio of conventional honeycombs approaches that of the matrix material as volume fraction approaches unity. The present FEM analysis used a plane stress assumption because it is physically more reasonable in actual honeycomb structures. Warren and Kraynik also adopted a plane stress approach. In the present analysis, however, we also examined the effect of the plane strain condition in honeycomb structures and then obtained the effective Poisson's ratio of honeycomb structures decreasing from 0.5 instead of unity. Under this condition, the three-dimensional stress state inside the matrix material prevents honeycomb structures from deforming laterally.

The variation of the effective Young's modulus of re-entrant honeycombs with an initial volume fraction of 0.1, with respect to the inverted angle of cell ribs, is described in Fig. 5. The effective Young's modulus of the present study for the re-entrant honeycomb has a similar tendency to that of Warren [7]. Gibson and Ashby treated the honeycomb structure orthotropically and obtained E_x, E_y by considering the bending of cell ribs only. When $\theta = -30°$ (regular hexagon), E_x was equal to E_y, which resulted in a transversely isotropic structure. This result, unrealistically, yielded a singular behaviour of Young's modulus as θ approached 0. E_x went to infinity because there were no bendable cell ribs at $\theta = 0°$. However, E_y decreased with the increase of the inverted angle of cell ribs.

The experimental results of three-dimensional foam materials showed that Young's modulus of the conventional foams was larger than that of the re-entrant foams. This does not correlate with Warren's result and the present FEM result. In the calculation of the effective moduli, the same method was applied as used by Warren and Kraynik [16] for the analysis of a three-dimensional foam, who obtained the effective elastic moduli by taking the average over all possible orientations. So, the re-entrant honeycomb structure has no preferred direction. It is treated as a transversely isotropic material, differing from Gibson and

Ashby's orthotropic approach. The two methods of Warren and Kraynik and Gibson and Ashby give the same result in the case of the conventional honeycomb with regular hexagons. However, the actual re-entrant honeycomb structure is not transversely isotropic, i.e. we cannot fill a plane isotropically with the re-entrant unit cells. Therefore, the present averaging technique does not properly account for the anisotropic property of the re-entrant honeycomb structure. As a result, it does not give a rigorous result for Young's modulus, as well as Poisson's ratio, of the re-entrant honeycomb structure. They are just an averaging moduli in the plane. Three-dimensional foams can be treated with this averaging process because foams have all possible orientations of unit cells and behave isotropically.

The second reason is that because of transforming from a convex polyhedron to a concave polyhedron in experiments for three-dimensional foams, the nodes of cell ribs and adjacent areas might have different material properties than those of original cell ribs. The change of material properties, of course, depends on the characteristics of the matrix materials. For example, non-linear elastic material or elasto-plastic material will give weaker nodes, which makes it easy to rotate cell ribs around the nodes rather than to bend cell ribs in the linear elastic region. However, a strain hardening material will result in stronger nodes. In this case, cell ribs will have almost fixed boundary conditions at the deformed nodes, whose linear elastic response is mainly composed of bending deformations of cell ribs with a shorter moment arm. The matrix materials of the three-dimensional foams used in experiments [2, 3] were polyurethane polymers which were non-linear elastic materials and copper which was almost an elasto-plastic material. Thus, the three-dimensional re-entrant foams might have weaker nodes, which resulted in lower Young's modulus than that in the conventional foams.

Fig. 6 shows the relationship between the effective Poisson's ratio and the inverted angle of cell ribs. The initial volume fraction of the re-entrant honeycomb is 0.1. The result of present study agrees well with Warren's [7] for the effective Poisson's ratio of the re-entrant honeycomb: a negative Poisson's ratio starts at $\theta = 12.3°$. But, Gibson and Ashby's result is for ν_{yx}, the negative ratio of strain in the x direction to that in the y direction, and it is slightly different to other results, as shown in Fig. 6 (a negative Poisson's ratio was expected at $\theta = 0°$). As in the case of the effective Young's modulus, Poisson's ratio ν_{xy}, the negative ratio of strain in the y direction to that in the x direction, goes to infinity as θ approaches 0, which is incorrect.

Materials with negative Poisson's ratios are a new concept and are not, at present, being utilized. However, there are many potential applications which take advantage of the negative Poisson's ratio itself, or the enhanced material properties. One possible application is that of composite sandwich panels. Sandwich panels are composed of stiff composite laminate skins of C- or glass-reinforced plastic sandwiching a light porous material, which may be one of the foams or

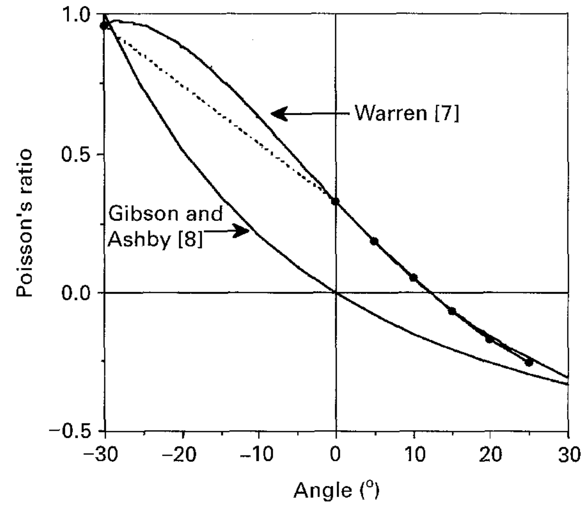

Figure 6 The relationship between the effective Poisson's ratio and the inverted angle of cell ribs with an initial volume fraction of 0.1; dotted line, no data available in the present results. ●, Present results.

honeycomb materials treated in this study. In the application of sandwich panels to aircraft bodies and wings, car doors and body panels, it should have a dome shape. Unfortunately, when a thick panel of the core material with a positive Poisson's ratio is curved downwards, its natural tendency is to curve up in the transverse direction, to form a saddle shape (anticlastic curvature). Currently, the only ways of making sandwich panels dome shaped are either by machining them or by forcing them into shape and damaging the core material. By using cores with a negative Poisson's ratio, useful dome-shaped sandwich panel (synclastic curvature) can be made easily.

The results of the present study are in good agreement with previous analytical results. In the next study, this homogenization FEM analysis will be applied to three-dimensional foam materials – conventional and re-entrant.

4. Conclusions

Based on the present FEM study using an homogenization technique, the following conclusions seem warranted. Matrix material properties do not significantly affect Poisson's ratio of the regular and re-entrant honeycomb structure. Young's modulus of the regular honeycomb structure increases with volume fraction. The regular honeycomb structure has a decreasing Poisson's ratio, from unity, with an increasing volume fraction. The re-entrant honeycomb structure has a negative Poisson's ratio and its value depends on the inverted angle of the cell edge. Young's modulus of the re-entrant honeycomb structure decreases with an increase in the inverted angle.

References

1. Y. C. FUNG, in "Foundation of solid mechanics" (Prentice-Hall, Englewood Cliffs, NJ, 1968).
2. J. B. CHOI and R. S. LAKES, *J. Mater. Sci.* **27** (1992) 4678.
3. *Idem., ibid.* **27** (1992) 5375.

4. A. G. KOLPAKOV, *Prikl. Mat. Mekh.* **59** (1985) 969.
5. R. F. ALMGREN, *J. Elasticity* **15** (1985) 427.
6. W. E. WARREN and A. M. KRAYNIK, *Mech. Mater.* **6** (1987) 27.
7. T. L. WARREN, *J. Appl. Phys.* **67** (1990) 7591.
8. L. J. GIBSON and M. ASHBY, in "Mechanics of Cellular Solids" (Pergamon Press, Oxford, 1988).
9. A. E. LOVE, in "A Treatise on the Mathematical Theory of Elasticity" (Dover Publication, NY, 1944).
10. M. MIKII and Y. MUROTSU, *JSME Int. J.* **32** (1989) 67.
11. K. E. EVANS, *J. Phys. D, Appl. Phys.* **22** (1989) 1870.
12. K. L. ALDERSON and K. E. EVANS, *Polymer* **33** (1992) 4435.
13. Z. HASHIN, *J. Appl. Mech.* **50** (1983) 481.
14. E. SANCHEZ de PALENCIA, in "Nonhomogeneous Media and Vibration Theory" (Lecture notes in physics, No. 127, Springer Verlag, Berlin, 1980).
15. J. M. GUEDES, PhD thesis, University of Michigan (1990).
16. W. E. WARREN and A. M. KRAYNIK, *J. Appl. Mech.* **55** (1988) 341.

Received 29 September 1994
and accepted 13 February 1996